The EMBO Journal (2009) 28, 663–676 | © 2009 European Molecular Biology Organization | Some Rights Reserved 0261-4189/09
www.embojournal.org

THE EMBO JOURNAL

EMBO open

A GLI1-p53 inhibitory loop controls neural stem cell and tumour cell numbers

Barbara Stecca[1] and Ariel Ruiz i Altaba*

Department of Genetic Medicine and Development, University of Geneva Medical School, Geneva, Switzerland

How cell numbers are determined is not understood. Hedgehog-Gli activity is involved in precursor cell proliferation and stem cell self-renewal, and its deregulation sustains the growth of many human tumours. However, it is not known whether GLI1, the final mediator of Hh signals, controls stem cell numbers, and how its activity is restricted to curtail tumourigenesis. Here we have altered the levels of GLI1 and p53, the major tumour suppressor, in multiple systems. We show that GLI1 expression in Nestin$^+$ neural progenitors increases precursor and clonogenic stem cell numbers *in vivo* and *in vitro*. In contrast, p53 inhibits GLI1-driven neural stem cell self-renewal, tumour growth and proliferation. Mechanistically, p53 inhibits the activity, nuclear localisation and levels of GLI1 and in turn, GLI1 represses p53, establishing an inhibitory loop. We also find that p53 regulates the phosphorylation of a novel N' truncated putative activator isoform of GLI1 in human cells. The balance of GLI1 and p53 functions, thus, determines cell numbers, and prevalence of p53 restricts GLI1-driven stem cell expansion and tumourigenesis.

The EMBO Journal (2009) **28,** 663–676. doi:10.1038/emboj.2009.16; Published online 12 February 2009
Subject Categories: development; molecular biology of disease
Keywords: brain; cancer; GLI1; p53; stem cells

Introduction

A key unresolved issue in biology is how cell numbers are determined during development, largely maintained in adulthood and deregulated in cancer. Hedgehog-Gli signalling is a key intercellular communication pathway involved in many aspects of development and cancer. During early brain development, it modulates precursor proliferation in different brain regions such as the neocortex, tectum and cerebellum (e.g., Dahmane and Ruiz i Altaba, 1999; Dahmane *et al*, 2001; Lien *et al*, 2006), while later on it regulates brain stem cell lineages (e.g., Lai *et al*, 2003; Palma and Ruiz i Altaba, 2004; Palma *et al*, 2005). It also drives rodent (Goodrich *et al*, 1997) and human (Dahmane *et al*, 2001) brain tumourigenesis and the self-renewal and survival of brain cancer stem cells (Clement *et al*, 2007). This dual involvement of Hh-Gli signalling in development and disease underlines its central role in controlling precursor cell numbers in the brain and other organs. It is not known, however, whether the level of GLI1 is critical to determine stem cell numbers and how GLI1 activity is restrained to prevent tumour formation.

Here we have tested two hypotheses: (1) GLI1 is a central determinant of stem cell numbers; (2) p53, the major human tumour suppressor, which regulates stem cell and precursor numbers (Gil-Perotin *et al*, 2006; Meletis *et al*, 2006), does so by negatively modulating the activity of GLI1. Testing these two ideas is important, as GLI proteins can integrate patterning and proliferative inputs in addition to HH signals (Brewster *et al*, 2000; Palma and Ruiz i Altaba, 2004; Kasper *et al*, 2006; Riobó *et al*, 2006; Dennler *et al*, 2007), as well as those from oncogenic RAS-MEK/AKT (Stecca *et al*, 2007); and p53 suppresses whereas GLI1 promotes tumourigenesis. We report that (1) the level of GLI1 determines the number of neural stem cells *in vivo*, (2) GLI1 and p53 act in an inhibitory loop, (3) endogenous GLI1 isoforms exist, and (4) a novel N'Δ GLI1 isoform is subject to regulation by phosphorylation in a p53-dependent manner. Our present and previous data suggest a critical regulation of GLI1 function in stem cell lineages by oncogenes and tumour suppressors, which is off-balance in disease.

Results

Elevation of GLI1 levels in neural progenitors results in a larger brain with expanded progenitor populations

To enhance Gli1 activity in stem cell lineages *in vivo*, we developed doxycycline (dox) inducible bigenic mice using the *Nestin* intron II driver (*Nestin->rtTA*-IRES-*LacZ* driver; Supplementary Figure 1), which is strongly expressed in embryonic neural progenitors but only very weakly postnatally (Figure 1; Supplementary Figures 1–4 and not shown). As a responder, we made a bidirectional GFP<-tetO->*myc-GLI1* transgene by random insertion (one line) or by targeting into the *hprt* locus (three lines). All bigenic lines showed the same phenotypes, and we focused on perinatal phenotypes of the first line resulting from sustained embryonic dox administration (Supplementary Table 1; Supplementary Figure 1).

Double-transgenic (DT)-treated mice (DT^{+dox}), but not untreated (DT^{-dox}) siblings or treated single transgenics, expressed GLI1 and GFP in precursors and displayed larger brains with hyperplasias of progenitor zones throughout from

*Corresponding author. Department of Genetic Medicine and Development, University of Geneva Medical School, 1 rue Michel Servet, 8242 CMU, Geneva CH-1211, Switzerland.
Tel.: +41 22 379 5646; Fax: +41 22 379 5962;
E-mail: Ariel.RuizAltaba@medecine.unige.ch
[1]Present address: Laboratory of Tumor Cell Biology, Core Research Laboratory—Istituto Toscano Tumori (CRL-ITT), Viale Morgagni 50, 50134 Florence, Italy

Received: 25 September 2008; accepted: 9 January 2009; published online: 12 February 2009

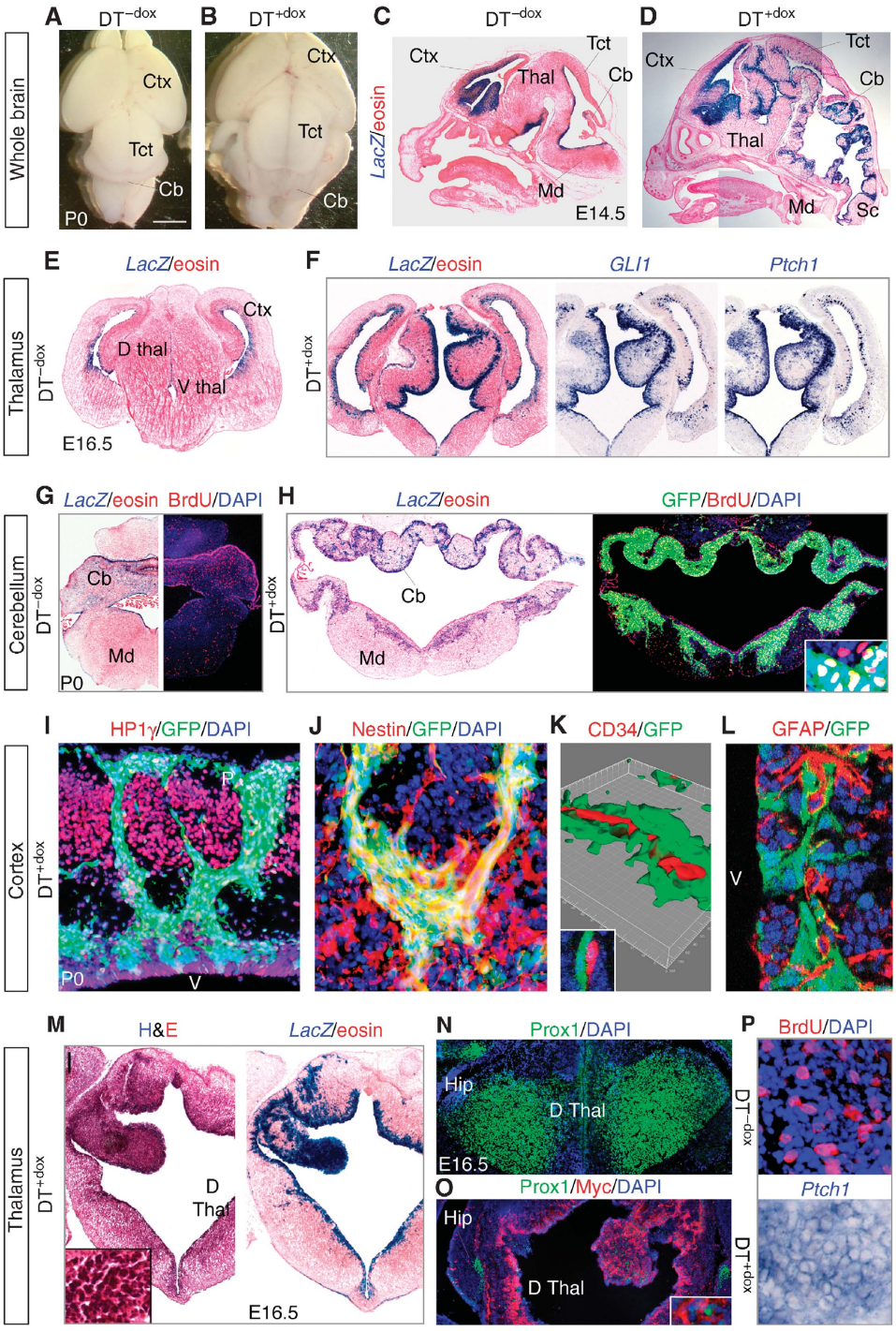

Figure 1 Enhanced GLI1 activity induces a larger brain with hyperplasias. (**A–D**) DT^{+dox} bigenic mice with strong phenotypes are perinatal lethal exhibiting a larger brain than DT^{-dox} siblings, seen dorsally (A, B) or in sagittal sections after Xgal staining highlighting the expression of the *Nestin->rtTA-LacZ* driver (C, D) (see Supplementary Figure 1). (**E–H**) Phenotypes detected in cross section in the thalamus (Thal; E, F), cerebellum (Cb) and medulla (Md; G, H) showing *LacZ* (Xgal) labelling (E–H), BrdU incorporation (G, H), *GLI1* and *Ptch1* (F) or GFP (H) expression in DT^{-dox} and DT^{+dox} siblings as indicated. (**I–K**) $HP1\gamma^{-}/Nestin^{+}/GFP^{+}$ precursors from the ventricle (v) invade the parenchyma through the cortical plate and expand near the pial (p) surface in the cingulate cortex (I, J). Invading GFP^{+} cells associate with $CD34^{+}$ endothelial cells in vessels as seen in a Z-stack confocal reconstruction (K) and a confocal image detail (K inset). (**L–P**) Phenotypic analyses in cross sections of subventricular zone of the lateral ventricle (SVZ) (L) and thalamus (M–P) for the markers indicated. Myc-GLI1 was mostly cytoplasmic and Prox1 nuclear (O inset). L shows a confocal image. Tissue is counterstained with eosin (e.g., C, D, M) and nuclei with DAPI (e.g., I, L). Hip, hippocampus; Sc, spinal cord; Tct, tectum; vz, ventricular zone; Scale bar = 1.5 mm (A, B), 1 mm (C, D), 0.5 mm (E–H), 100 μm (O inset, J, P), 200 μm (I), 70 μm (L; H inset), 14 μm (K), 10 μm (K inset), 0.6 mm (M, N, O), 150 μm (M inset).

forebrain to spinal cord (Figure 1A–D; Supplementary Figure 1 and not shown). The strength of the phenotype varied within a litter. DT^{+dox} mice with a strong phenotype (Figure 1) were embryonic lethal or died shortly after birth. Surviving animals had milder alterations (Supplementary Figure 3A). Three brain regions with strong phenotypes (cortex, thalamus and cerebellum) and the spinal cord had high levels of *LacZ*, GFP and Nestin and of *GLI1* and

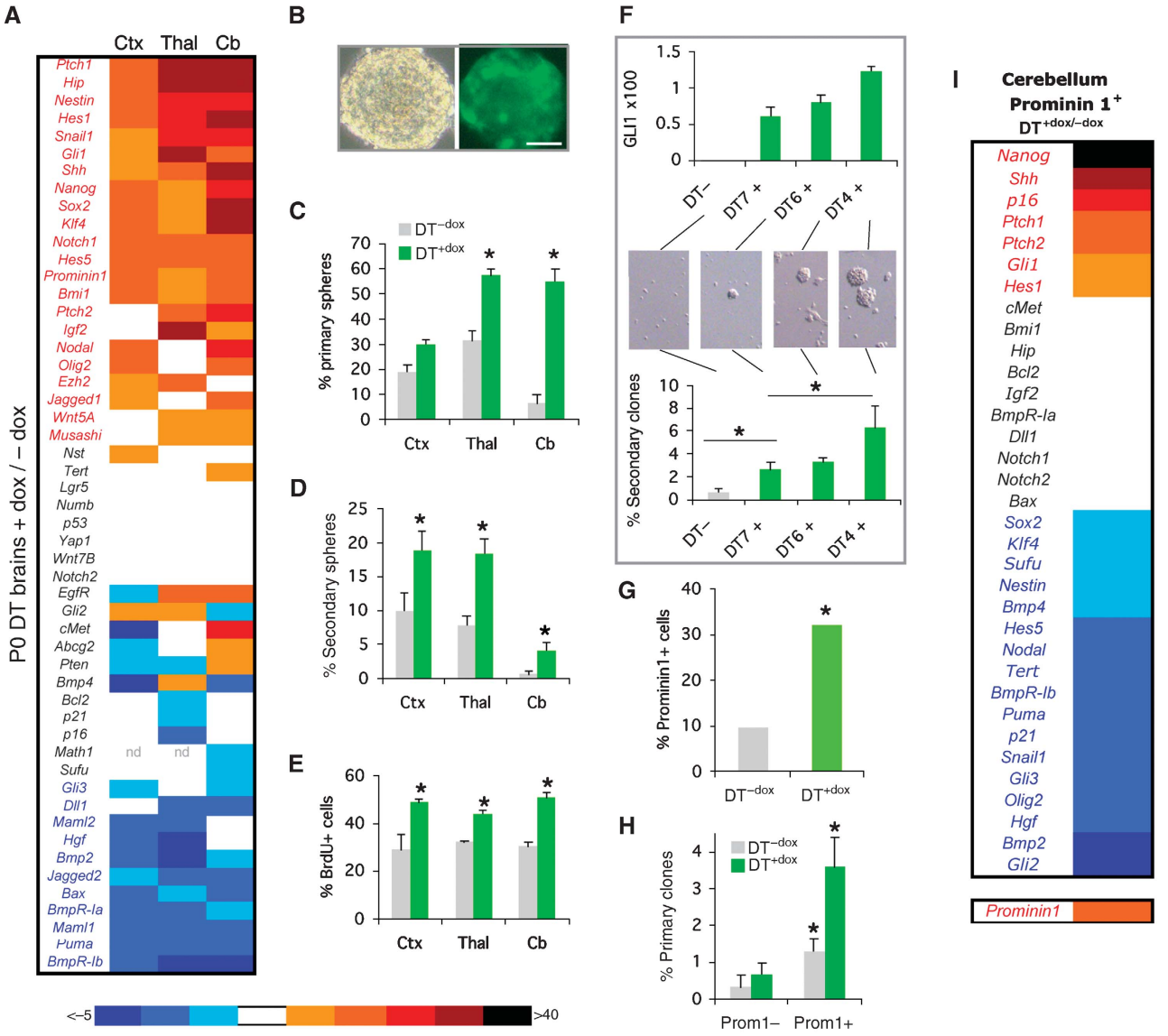

Figure 2 Gene expression and cellular behaviour in neurospheres and stem cells. (**A**) RT–qPCR analyses of P0 dissected tissues from cortex (Ctx), thalamus (Thal) or cerebellum (Cb). qPCR values in all panels reflect ct values after normalisation with the geometrical mean of the values of *Gapdh*, *βactin* and *EFIα* and shown as the DT^{+dox}/DT^{-dox} value ratios. See Supplementary Figure 5. (**B**) Phase contrast and fluorescence images of DT^{+dox} NS. (**C**–**E**). Histograms of the number of neurospheres (C, D) or $BrdU^+$ cells (E) as indicated. Primary spheres were quantified per 250 000 brain cells. (**F**) The level of *GLI1* determines NS numbers. *GLI1* expression values and secondary sphere number were determined for the same samples. (**G**–**I**) Quantification of the number (G), clonogenicity after MACS (H) and gene expression analyses (I) by RT–qPCR of $Prominin1^+$ cerebellar stem cells (see Supplementary Figure 6B). Here and in all figures asterisks denote significative changes ($P<0.05$) and error bars are s.e.m. Scale bar = 80 μm (B).

endogenous *Ptch1* mRNAs in progenitor cells (Figure 1E–H, M and P; Supplementary Figures 2–4). The cerebellar external germinal layer, which has the highest levels of endogenous *Gli1* (Dahmane and Ruiz i Altaba, 1999), was largely unaffected, whereas the ventricular zone (VZ) was hyperplastic (Figure 1G and H; Supplementary Figure 3A, B). The tectum (colliculi) was also larger but did not show convoluted tissue as the cerebellum, thalamus or medulla (Figure 1A–D; Supplementary Figure 1). Massive and highly invasive precursor hyperplasias were also detected in the spinal cord (Supplementary Figure 4).

Transgenic *GLI1* induced ~4–13-fold the activity of the endogenous Hh-Gli pathway as assessed by the increased expression of *Gli1* and *Ptch1* (Figure 2A; Supplementary Figure 5). It also boosted 2–8-fold BrdU incorporation in a region-specific manner (Figure 1G, H and P; Supplementary Figure 2C, D, G, H). In the cortex and subventricular zone of the lateral ventricle (SVZ), we found high GFP^+, $LacZ^+$, $Ptch1^+$, myc-$GLI1^+$ groups of cells streaming from the VZ to the pial surface (Figure 1I and J; Supplementary Figure 2A–E, I). These cells were $HP1\gamma^-$, a heterochromatin (neuronal and senescent cell) marker (Figure 1I); they expressed high levels of Nestin (Figure 1J; Supplementary Figure 2B, E), associated with $CD34^+$ vessels (Figure 1K) similarly to human gliomas (Farin *et al*, 2006), and derived from $Nestin^+$, $GFAP^-$ VZ cells (Figure 1L).

DT^{+dox} GFP^+ regions in thalamus and cerebellum showed the highest proliferative levels (Figure 1G and H; Supplementary 2G, H) with reduced (2–3-fold) apoptosis (Supplementary Figure 3C). Massive, tumour-like hyperpla-

sias with high nuclear density, GFP, *LacZ* and *Ptch1* expression were prominent in these regions (Figure 1F, H and M). Hyperplasias showed little differentiation as assessed, for instance, by exclusion of neuronal Prox1 (Figure 1N and O), neuroblast *NeuroD1* staining in dorsal thalamus (Supplementary Figure 3D), or astrocytic GFAP expression in cerebellum (not shown). A slight increase in the expression of the oligodendrocyte progenitor marker *Pdgfrα* was detected in thalamus (Supplementary Figure 3D). Unaffected regions preserved differentiation (Supplementary Figure 2J). As the strong phenotype is perinatal lethal, and we found that transgenes are silenced ~1–2 weeks after birth, it is unclear whether such lesions could develop into frank tumours.

GLI1 upregulates an embryonic stem cell signature in the brain and modulates different signalling pathways

Gene expression analyses by qPCR of different regions of perinatal DT^{+dox} brains showed that GLI1 induced Shh-Gli pathway components and targets including *Shh*, *Gli1*, *Hip*, *Ptch1*, *Snail1 and Igf2* (Figure 2A; Supplementary Figure 5). It also upregulated a group of 'stemness' genes, including *Nanog*, *Sox2*, *Klf4*, *Nestin*, *Prominin1 (CD133)* and *Bmi1* (Figure 2A), which is reminiscent of that of human gliomas (Clement *et al*, 2007). The changes in gene expression levels were greatest in the cerebellum, consistent with phenotype strength (Figure 1; Supplementary Figures 1–4), although each region displayed overlapping yet context-dependent signatures. DT^{+dox} brains also showed an increase in Notch (*Hes1*, *Hes5*, *Notch1*, *Jagged1*) and the repression of BMP (*Bmp2*, *Bmpr-Ia*, *Bmpr-Ib*) activity signatures (Figure 2A), with *Bmpr-Ia* and *-Ib* being key determinants for stem cell responses to BMPs (Panchision *et al*, 2001). Enhanced GLI1 may thus increase the number of $Nestin^+$ stem cells reflected in the upregulation of stemness genes involving modification of Notch, BMP and other (Igf2, Nodal, Hgf; Figure 2A) signalling pathways.

GLI1 induces an increase in the number of clonogenic neural stem cells

Given the lack of unequivocal neural stem cell markers *in vivo*, we tested for stem cell behaviour. Different parts of DT^{+dox} brains showed an increase in the number of primary and secondary clonal stem cell-derived neurospheres (NS), as compared with DT^{-dox} brains, displaying a concomitant increase in proliferation with unchanged apoptosis levels (Figure 2B–E and not shown). DT^{-dox} and DT^{+dox} NS remained multipotent and DT^{+dox} produced 2–5-fold more neurons than DT^{-dox} NS upon differentiation (Supplementary Figure 6A). Efficient NS formation from the cerebellum was only obtained from DT^{+dox} mice (Figure 2C and D).

Importantly, we found a direct correlation between the number of NS formed from single DT^{+dox} cerebella and the level of *GLI1* (Figure 2F) so that higher levels of GLI1 produced more NS. To further address the role of GLI1 in stem cells *in vivo*, we analysed the number of stem cells expressing Prominin1 (Lee *et al*, 2005) by MACS sorting DT^{+dox} and DT^{-dox} cerebella. The number of cerebellar $Prominin1^+$ stem cells *in vivo* increased ~3-fold in DT^{+dox} over DT^{-dox} (Figure 2G), showing the *in vivo* enhancement of stem cell numbers by GLI1. As expected, the $Prominin1^+$ fraction showed 4–6-fold increased clonogenicity over $Prominin1^-$ cells (Figure 2H).

Gene expression signatures of purified $Prominin1^+$ stem cells from DT^{+dox} and DT^{-dox} E17.5 cerebella revealed an enrichment of *Gli1*, *Shh*, *Ptch1*, *Ptch2*, *Nanog* and *Hes1* and low expression of BMP signalling components in DT^{+dox} stem cells (Figure 2I; Supplementary Figure 6B), showing an action of GLI1 in stem cells. Gene expression analyses of whole E17.5 NS further supported the findings with dissected brain and purified $Prominin1^+$ stem cells, although a number of genes showed variant expression (Supplementary Figure 5), probably reflecting different cellular compositions.

Cooperation of GLI1 and p53 knock-down on neural stem cell self-renewal and tumour growth

The downregulation of *p21* and *Puma*, two p53 targets, in $Prominin1^+$ stem cells of DT^{+dox} cerebella (Figure 2I) is consistent with the finding that p53 negatively controls neural stem cell numbers (Gil-Perotin *et al*, 2006; Meletis *et al*, 2006). Because the perinatal lethality of DT^{+dox} mice with strong phenotypes prevented us from analysing DT^{+dox};$p53^{-/-}$ mice for the possible development of frank tumours and further expansion of stem cell pools, we first tested for the role of p53 on GLI1-induced NS self-renewal.

E17.5 cortical and thalamic DT^{-dox} and DT^{+dox} NS, or wt NS transduced with control or GLI1-expressing lentivectors were further transduced with a control or an shRNA specific for p53 (shp53). Enhanced GLI1 or knock-down (kd) of p53 increased the number of clones as expected, but importantly, their simultaneous action was synergistic (Figure 3A). They also increased proliferation and decreased apoptosis additively (Figure 3B and C). Wt postnatal SVZ NS transduced with lentivectors expressing full-length *GLI1* or *shPtch1* (to endogenously enhance the Shh-Gli1 pathway) alone and in combination with shp53 yielded similar synergism in clonogenicity and additive results in proliferation and apoptosis (Figure 3D–F). p53 therefore antagonises GLI1 in the control of neural stem cell self-renewal in NS of different brain regions.

Following these findings, we tested whether enhanced GLI1 cooperates with p53 kd in tumour growth. As all patient-derived glioblastoma stem cell cultures that efficiently grew in our hands were p53 mutant (M Vucikevic and ARA, personal communication), and as NS from DT^{+dox} mice extinguished transgene expression *in vivo* after transplantation (not shown), we used human U87 glioblastoma (p53 wt) cells. These cells show the least number of genomic changes among glioma cell lines (Li *et al*, 2008). Cells transduced with lentivectors expressing GLI1 or GLI1 plus shp53 were grafted intracranially and tumours removed when the mice showed signs of neurological disease. Enhanced GLI1 expression induced an acceleration of tumour development (Figure 3G and H) and an increase in tumour weight as compared with controls. p53 kd alone did not accelerate tumour development, but it synergised with enhanced GLI1 levels (Figure 3G and H). These results are consistent with the acceleration of cerebellar tumours in $Ptc1^{+/-}$;$p53^{-/-}$ mice as compared with *Ptc1+/−* siblings (Wetmore *et al*, 2001), although the bases of such acceleration is unknown.

Balancing SHH-GLI and p53 activities in the control of tumour cell numbers

As expected, kd of HH-GLI signalling with a validated shSMOH (Clement *et al*, 2007; Stecca *et al*, 2007) or with

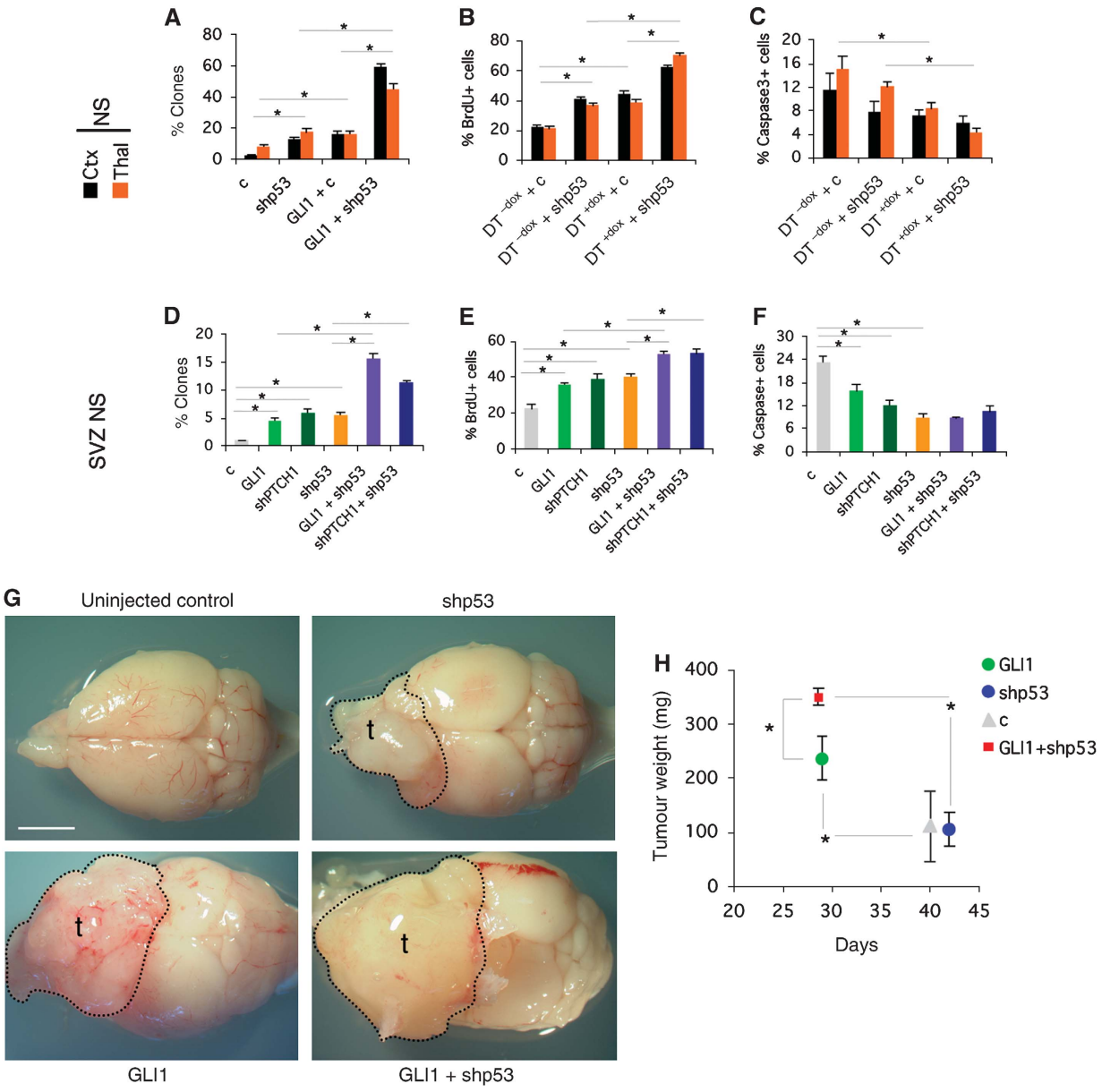

Figure 3 Synergistic control of neural stem cell self-renewal and xenograft growth by GLI1 and kd of p53. (**A–F**) Quantification of the behaviour of E17.5 NS from cortex (Ctx) or thalamus (Thal) (A–C) or of first week postnatal SVZ NS (D–F) testing for clonogenicity (A, D), proliferation (B, E) and apoptosis (C, F). Cells were derived from DT mice and treated as indicated or were wt NS transduced with lentivectors as shown. (**G**) Dorsal views of mouse brains uninjected or injected with transduced U87 cells as indicated. Tumour contours (t) are denoted. (**H**) Quantification of tumour weights versus time after injection; $n = 5$ for each condition. c = control lentivector. Scale bar = 0.4 mm (G).

validated 21-nt siRNAs against GLI1 (siGLI1; Sanchez *et al*, 2004; Stecca *et al*, 2007) decreased U87 cell proliferation and enhanced apoptosis (Figure 4A–C). In contrast, p53 kd increased proliferation of U87 cells (Figure 4A and B). Interestingly, epistatic analyses revealed that shp53-enhanced proliferation was blocked by both shSMOH and siGLI1 but not by control lentivectors or control siRNAs (Figure 4A and B) on the one hand, whereas on the other, cell death induced by shSMOH was blocked by shp53 (Figure 4C), suggesting mutual requirement.

Consistent with this idea, restoration of p53 function in p53-mutant brain tumour cells (U251 glioma and Daoy medulloblastoma) reduced, and enhancement of GLI1 levels increased, their proliferation, but these effects were mutually compensated (Figure 4D). Similarly, oxaliplatin treatment of U87 cells increased endogenous p53 levels through the DNA damage response and decreased cell proliferation (Figure 4E), but this proliferative defect and the level of induced phospho-p53 were attenuated in cells with enhanced GLI1 levels (Figure 4E), further suggesting a balance of levels and activities. Enhanced GLI1 levels, however, also induced hallmarks of DNA replication stress (Gorgoulis *et al*, 2005) that are known to lead to enhanced p53 function in different scenarios: increasing the number of 53BP1 protein foci in 293T cells and increasing the number of phospho-Chk2$^+$ cells in DT^{+dox} hyperplastic thalamic and cerebellar regions (Supplementary Figure 7A, B). Together, these data suggest an endogenous antagonistic relationship between p53 and GLI1 but also the possible induction of p53 function by GLI1 through the DNA replication stress response.

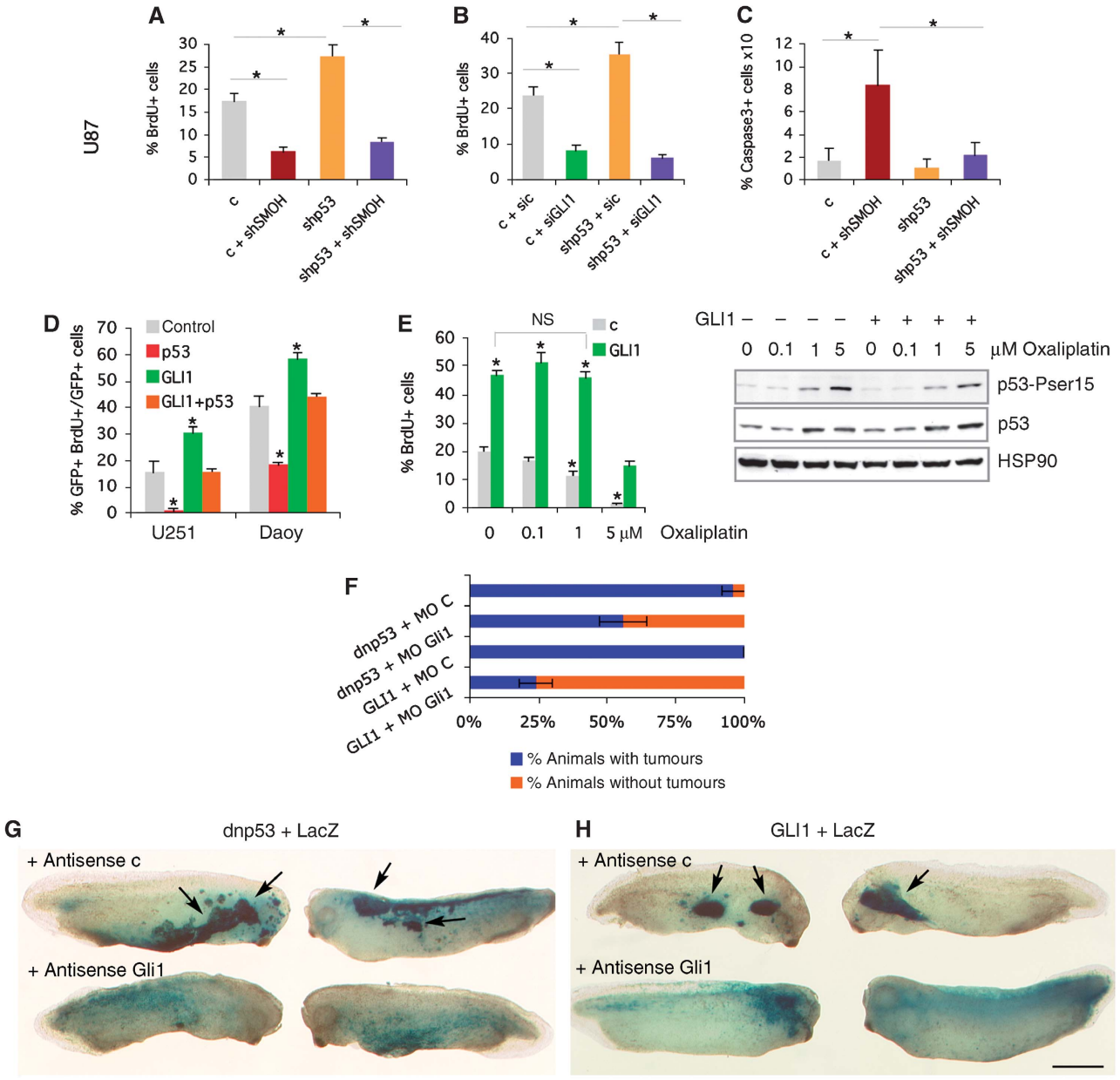

Figure 4 Mutual requirements of p53 and GLI1 in proliferation and apoptosis. (**A**–**C**) Histograms of the changes in cell proliferation (A, B) or apoptosis (C) after altering SMOH, GLI1 or p53 levels by lentiviral transduction or siRNA lipofection in U87 cells. (**D**) Compensatory effects in cell proliferation in U251 and Daoy cells by GLI1 and p53. (**E**) Left: Rescue of the anti-proliferative effect of p53 induction by oxaliplatin (48 h) by transduced GLI1 in U87 cells. Comparisons are with untreated (0) control (c) except where noted. Right: Western blot of the levels of p53 and phospho-serine15 p53 induced by oxaliplatin with or without exogenous GLI1. Hsp90 is used as control. (**F**–**H**) Quantification (F) and whole-mount side views (G, H) of Xgal-stained stage 32 tadpoles facing the centre of each panel with epidermal hyperplasias (arrows; top rows, G, H) or the normal distribution of cells in the epidermis (bottom rows, G, H) as indicated. Scale bar = 0.6 mm (G, H).

Epidermal hyperplasias induced by interference with p53 function require endogenous Gli1

The blockade of shp53-mediated increased cell proliferation by interference with endogenous SMOH or GLI1 function (Figure 4A and B) suggested that interference with p53 frees endogenous GLI1 from negative regulation, leading to cell overproliferation. As an *in vivo* assay to analyse this idea, we tested for the role of Gli1 in tumours induced by blockade of p53. Frog embryos expressing dominant negative (Thr^{280}) p53 (dnp53), which inhibits endogenous p53 function, develop epidermal tumours (hyperplasias) (Wallingford *et al*, 1997). Co-injection of a control antisense morpholino oligonucleotide (MO) along with dnp53 did not modify its tumour-inducing activity ($n = 18/19$ tadpoles with tumours; Figure 4F–H). In contrast, coinjection with a proven MO specific for frog *Gli1* (Dahmane *et al*, 1997, 2001; Nguyen *et al*, 2005) reduced the development of dnp53-induced tumours by ~40% ($n = 21/37$). As a control for MO specificity, injection of *Gli1* MO ($n = 6/24$), but not the control MO ($n = 27/27$), reduced tumour development by co-injected human *GLI1* by 66% (Figure 4F–H; Dahmane *et al*, 1997, 2001; Nguyen *et al*, 2005). Blockade of endogenous *Gli1* changed the distribution of the descendants of the injected blastomeres from clumped in tumours to evenly in the epidermis, appropriate for the normal fate of the injected

blastomeres (Figure 4G and H). Enhanced GLI1 function (through injection) therefore bypasses proliferative restrictions imposed by p53, and blockade of endogenous p53 unleashes the proliferative activity of endogenous Gli1.

p53 negatively regulates the activity, nuclear localisation and levels of GLI1

Gene expression analyses of NS expressing both GLI1 and shp53 revealed context-specific differences in the effect of p53 kd on GLI1-regulated genes (Supplementary Figure 8), for instance, increasing the expression of the stemness genes *Prominin1*, *Bmi1* and *Nanog*, as well as *p16*, *Gli1*, *Hes1*, *Hes5* and other Notch components in different regions, whereas decreasing *p21* in cortex and cerebellum, all as compared with NS expressing GLI1.

To elucidate how p53 alters the genetic program induced by GLI1, we first asked whether p53 affects GLI1-dependent transcription in GLI-dependent luciferase reporter assays. shp53 increased 2–3-fold the activity of GLI1 in wt postnatal mouse SVZ NS, and this was reproduced in human U87 and in 293T cells (Figure 5A and B; Supplementary Figure 9A). dnp53 behaved similarly and p53 kd also augmented the diminished activity of N'Δ forms of GLI1 and GLI2 (Figure 5A). shp53 did not endow GLI3 or its C'Δ repressor form (GLI3R) with activity (Figure 5A; Supplementary Figure 9A), suggesting that it does not act by inhibiting repressor function. Conversely, restoring p53 activity in U251 and Daoy cells (both p53 mutant) decreased GLI1 reporter activity and the levels of exogenous GLI1 in a concentration-dependent manner (Figure 5C; Supplementary Figure 9B). p53 did not affect the levels of *GLI1* mRNA in co-transfected cells (not shown). Enhanced transcriptional activity by shp53 was correlated with two-fold enhanced nuclear localisation of GLI1, of N'Δ forms of GLI1 and GLI2 but not of GLI3, GLI3R or of a nuclear targeted NLS-Gli1 (Ruiz i Altaba, 1999; Figure 5D and E). p53 thus appears to promote the localisation of GLI1, and possibly of GLI2, in the cytoplasm, where it can be degraded by the proteasome (Huntzicker *et al*, 2006).

To test whether p53 generally inhibits GLI1 levels, we analysed GLI1 protein in different contexts. E17.5 thalamic NS of DT^{+dox} brains were transduced with control or shp53 lentivectors and kept in the presence of dox. Western blots with a commercial anti-GLI1 antibody (α-$GLI1^{\sim 420}$; Cell Signalling) showed that p53 kd induced a 30% increase in full-length GLI1 (>160 KD) and a three-fold increase of a shorter form running ±130 KD (Figure 5F), quantified by densitometry. Similarly, analysis of postnatal wt SVZ NS for endogenous mouse Gli1 with an anti-GLI1 antibody to the C-terminus (α-$GLI1^{803-818}$; GeneTex) showed a 40% increase in full-length mouse Gli1 (>160 KD) and a 2.3-fold increase in a shorter form running at ~115 KD (Figure 5G). As control, and as α-$GLI1^{\sim 420}$ does not recognise mouse Gli1 (Figure 6C), we used α-$GLI1^{803-818}$ to probe extracts of P10 wt cerebellum, adult (~4 mo) Cb and a $Ptch1^{+/-};p53^{-/-}$ medulloblastoma (MB) (Figure 5H). As expected from the transient perinatal expansion of cerebellar $GLI1^{+}$ granule neuron progenitors and the strong expression of *GLI1* in MB (Dahmane and Ruiz i Altaba, 1999; Dahmane *et al*, 2001), the full-length and the shorted 115 KD form were clearly detected at P10 and were nearly undetectable in adult cerebellum, whereas the full-length form was 14-fold and the 115 KD form 6.5-fold more abundant in MB than at P10 (Figure 5H).

GLI1 represses p53

The mutual compensatory effect of GLI1 and p53 (Figure 4D) and the dominance of GLI1 kd over p53 kd (Figure 4B) raised the possibility that in addition to the negative regulation of GLI1 by p53, p53 itself could be under GLI1 regulation. Analyses of p53 in GLI1 kd cells (see below) revealed that endogenous p53 is under the control of endogenous GLI1 as assessed by the levels of total p53 and of active phospho-serine15 p53 (p53-P) in cells lipofected with siGLI1 versus siC (Figure 6E). The kd of endogenous GLI1 function increased p53 ~5-fold and phospho-serine15 p53 ~2-fold. This indicates that in addition to the inhibition of GLI1 by p53 described earlier, endogenous GLI1 regulates the levels of endogenous p53, suggesting a negative regulatory loop.

Enhanced GLI1 levels can inhibit p53 regulation *in vitro* through the activation of the p53 inhibitor Hdm2 (Abe *et al*, 2008). We find that Mdm2, the mouse homologue of Hdm2, is greatly enhanced in DT^{+dox} versus DT^{-dox} brains (Figure 6F), extending this possible mechanism of action to an *in vivo* context.

The inhibitory loop between GLI1 and p53 is consistent with the inversely reciprocal levels of GLI1 and p53 observed in two primary glioblastoma stem cell cultures (Figure 6G; Clement *et al*, 2007). The level of GLI1 correlated with their proliferation rate (Figure 6G). GBM12 harbours a *p53* gene with a frameshift mutation corresponding to aa 209 (M Vukicevic and ARA, unpublished) and predicted to encode an unstable protein as no p53 or phospho-serine15 p53 proteins were detected (Figure 6G). GBM13 expresses full-length p53 with an R->H substitution at aa 158 within the DNA-binding domain (M Vukicevic and ARA, unpublished) predicted to yield a protein with compromised transcriptional activity (Kato *et al*, 2003). Whereas full-length GLI1 protein was barely detectable (not shown), GMB12, which has no p53, showed higher levels of $GLI1^{130}$ (see below) than GBM13, which expresses p53 with reduced activity.

Identification of human GLI1 isoforms

Given the existence of isoforms of GLI1 (Figure 5F–H), reminiscent of those of other Gli proteins, we investigated the possibility that p53 affects their formation or function in human cells. Transfection of U251 glioma cells with full-length myc-tagged GLI1 (Figure 6A, left) revealed the full-length form running at >160 KD ($GLI1^{FL}$) plus one predominant smaller N-terminal tagged form running at ~110 KD ($GLI1^{110}$) after probing the western with α-N' myc tag antibodies. This form has been proposed to act as a C'Δ repressor (Ruiz i Altaba, 1999). Treatment with cycloheximide to block *de novo* protein synthesis showed increased stability of $GLI1^{100}$ over $GLI1^{FL}$ (Figure 6A, left). The production of distinct GLI1 isoforms could be limiting in different cells or context dependent as GLI1 transfected in U87 cells yielded the full-length protein but only traces of smaller products (Supplementary Figure 9C). This variance also suggests that the stable products seen in U251 are not non-specific, ubiquitous degradation products.

To directly monitor GLI1 isoforms, we developed an affinity-purified, specific antibody (α-$GLI1^{412-427}$) against a domain immediately C-terminal to the zinc fingers of human

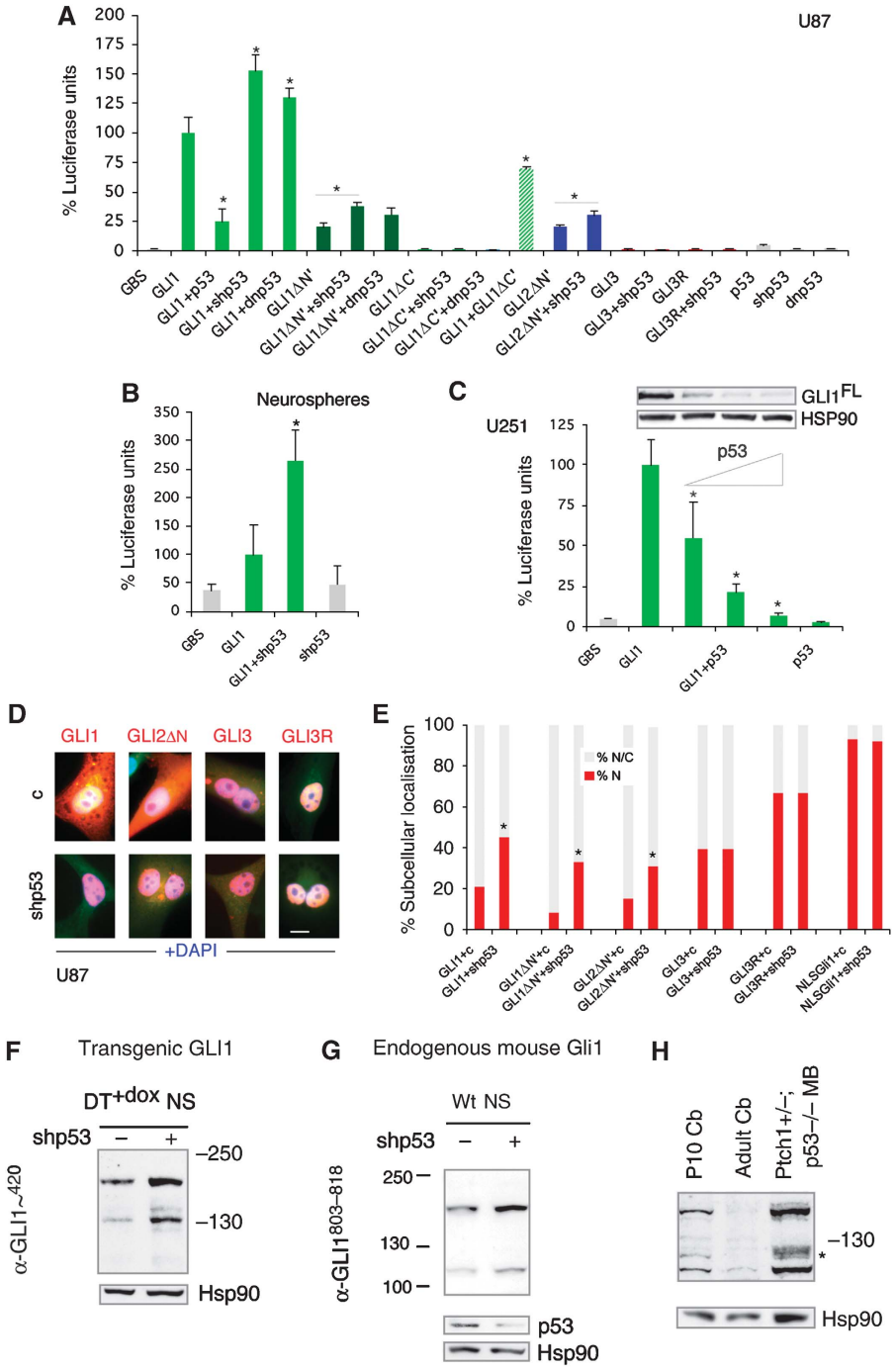

Figure 5 Regulation of GLI1 by p53. (**A**–**C**) Quantification of GLI-dependent luciferase reporter assays (A–C) and inhibition of $GLI1^{FL}$ by p53 (C). Luciferase units are GLI reporter firefly/renilla control ratios with the level induced by GLI1 equated to 100%. p53 was used at 1/0.25, 1/0.5, 1/1 maintaining equal amounts of GLI1 (triangle in C). (**D**, **E**) Representative images (D) and quantification of GLI nuclear localisation in U87 cells (E). (**F**–**H**) Western blots showing the expression of transgenic GLI1 in thalamic DT^{+dox} NS (F), endogenous Gli1 in postnatal SVZ NS (G) and endogenous Gli1 in P10 and adult cerebella as well as in a *Ptch1*$^{+/-}$;*p53*$^{-/-}$ medulloblastoma (MB; H). Transduction with shp53 lentivectors leads to an increase in the abundance of transgenic GLI1 (F) and endogenous Gli1 (G). p53 and Hsp90 are used as controls. Scale bar = 15 μm (D).

GLI1 that we had previously targeted (Dahmane *et al*, 1997). Reprobing the anti-myc tag westerns in human U251 cells with α-GLI1 revealed the same full-length and 110 KD isoforms plus a novel ~130 KD form at similar exogenous levels (Figure 6A, right). This form lacks the myc tags and thus the N-terminus. Endogenous GLI1 was expressed at much lower levels (see below). Treatment with cycloheximide showed differential isoform stability: $GLI1^{130}$ peaked at 1 h, $GLI1^{100}$ was largely stable with a 1.6-fold increase at 4 h, and $GLI1^{FL}$ decayed 2.4-fold at 4 h (Figure 6A, right). As the 130 KD N'Δ species cannot give rise to the ~100 KD C'Δ form, this suggests a precursor-product relationship between the $GLI1^{FL}$ and the $GLI1^{130}$ form and between $GLI1^{FL}$ and $GLI1^{100}$ (Figure 6B), with $GLI1^{100} > GLI1^{130} \gg GLI1^{FL}$ stabilities, arguing against the first two being non-specific degradation products.

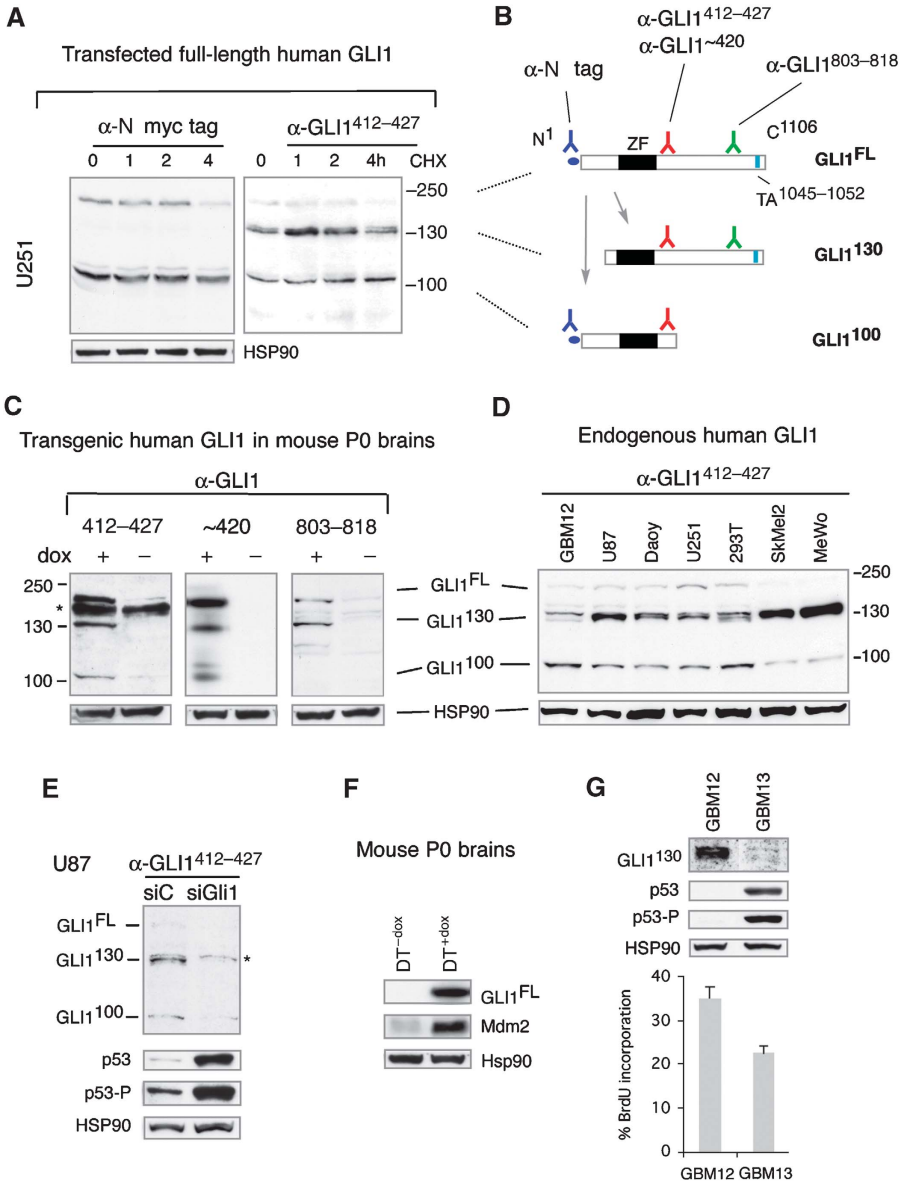

Figure 6 GLI1 protein isoforms and endogenous repression of p53 by GLI1. (**A**) Transfected myc-GLI1 isoforms detected as indicated in samples treated with cycloheximide (CHX) as shown. $GLI1^{FL}$ migrates >160 KD. (**B**) Deduced relationship of $GLI1^{130}$ and $GLI1^{100}$ to $GLI1^{FL}$, and location of Ab epitopes and of the transactivating (TA) domain. (**C**) Analyses of human GLI1 protein in transgenic P0 mice as indicated. All three antibodies used recognise $GLI1^{FL}$ and $GLI1^{130}$, but only those to the domain immediately C-terminal to the zinc fingers (ZF in B) recognise $GLI1^{100}$. (**D**) Analysis of GLI1 isoforms in human cell lines and in a GBM stem cell culture (gliomasphere). (**E**) GLI1 kd with a specific siRNA for 8 h, but not a control siRNA, depletes all three isoforms in U87 cells, while enhancing total and phospho-serine15 p53 (p53-P) levels. Non-specific bands are denoted by asterisks. (**F**) Levels of Mdm2 in the blot shown in panel C middle for GLI1 and Hsp90. (**G**) Comparison of the levels of $GLI1^{130}$, p53, phospho-serine15 p53 and HSP90 in two gliomaspheres that proliferate at different rates.

To further characterise the structure of the isoforms, we used two commercial polyclonal antibodies against GLI1: α-$GLI1^{\sim 420}$ made to the same region as our α-$GLI1^{412-427}$ and the C-terminal antibody α-$GLI1^{803-818}$. Western blots of P0 DT^{+dox} and DT^{-dox} brain extracts revealed the presence of $GLI1^{FL}$, $GLI1^{130}$ and $GLI1^{100}$ only after induction with dox with α-$GLI1^{412-427}$ and α-$GLI1^{\sim 420}$, confirming specificity (Figure 6C). α-$GLI1^{412-427}$ also picked up a non-specific band in mouse brain extracts (asterisk, Figure 6C). In contrast, α-$GLI1^{803-818}$ picked up $GLI1^{FL}$ and $GLI1^{130}$ but not $GLI1^{100}$ (Figure 6C) (and minor background bands), consistent with the C' truncation of $GLI1^{100}$ and the N' truncation of $GLI1^{130}$ (Figure 6B). Probing with a different polyclonal C-terminal antibody (α-$GLI1^{805-820}$; Chemicon) made to the same region gave the same results (not shown).

To analyse whether endogenous human GLI1 isoforms exist, we probed western blots of U87 cells that are known to harbour an active HH-GLI pathway (Clement *et al*, 2007) with our own and seven commercial α-GLI1 antibodies (see Materials and methods). Only α-$GLI1^{412-427}$ yielded the expected pattern of endogenous isoforms (Figure 6D; Supplementary Figure 9D and not shown) seen previously (Figure 6A and C). The other antibodies revealed various non-consistent patterns (not shown). Thus, whereas many α-GLI1 antibodies recognise enhanced levels of GLI1, only α-$GLI1^{412-427}$ recognises endogenous human GLI1.

Analysis of a patient-derived glioblastoma stem cell culture (GMB12; Clement *et al*, 2007) and a panel of human tumour cell lines with α-GLI1$^{412-427}$ revealed all isoforms with GLI1^{130} > GLI1^{100} > GLI1^{FL} abundances (Figure 6D). GLI1^{130} was most prevalent in metastatic melanomas (which harbour active GLI1; Stecca *et al*, 2007), and it was consistently detected as a doublet (Figure 6D). Endogenous human GLI1^{FL} and GLI1^{100} do not have N' myc tags and are therefore slightly smaller than their tagged exogenous counterparts (Figure 6A and C). Commercial westerns further confirmed the presence of a GLI1 ~130 KD form in various human tissues and tumours with a possible tumour-specific alteration in GLI1 (Supplementary Figure 9E, F).

To verify the identity of the isoforms recognised by α-GLI1$^{412-427}$, we used RNAi to kd endogenous GLI1. Lipofection of a specific siRNA previously proven to target *GLI1* mRNA (siGLI1; Sanchez *et al*, 2004; Clement *et al*, 2007; Stecca *et al*, 2007) but not of a control siRNA (siC), knocked-down GLI1^{FL} two-fold, GLI1^{130} 13-fold and GLI1^{100} 4.4-fold. The levels of HSP90 were unaltered (Figure 6E).

Constructs that approximate the GLI1 N'Δ and C'Δ isoforms have divergent functions

To address the possible functional significance of GLI1 isoforms, we analysed the activity of GLI1 constructs that approximate N'Δ GLI1^{130} and C'Δ GLI1^{100} (GLI1N'Δ and GLI1C'Δ; Ruiz i Altaba, 1999). Consistent with the presence of the transcriptional activation domain close to the C-terminus (Figure 6B; Yoon *et al*, 1998), these constructs behaved as weak activators or repressors, respectively, in GLI1-dependent reporter assays (Ruiz i Altaba, 1999) (Figure 5A). The strength of GLI1N'Δ activator was context dependent, as its activity was 1.2-fold weaker than GLI1^{FL} in melanoma SkMel2 cells but 3.4-fold stronger in prostate cancer LNCaP cells (not shown), and similarly or more active in other cell types (Yoon *et al*, 1998; Sasaki *et al*, 1999).

p53 and HH signalling regulate the status of GLI1^{130}

The existence of GLI1 isoforms raised the possibility that p53 could alter their genesis or levels. Treatment of U87 cell extracts *in vitro* with λ phosphatase followed by western blotting with α-GLI1$^{412-427}$ revealed the conversion of the upper band of the GLI1^{130} doublet to the lower one (Figure 7A and D), indicating that the upper band is a phosphoform of GLI1^{130} (GLI1^{130P}). GLI1^{100} decreased slightly but did not change size (Figure 7A), and the GLI1^{FL} band became fainter (Figure 7A and not shown), suggesting that it might also be affected although its rarity made further assessment not possible. Consistently, however, the level of exogenous GLI1^{FL} decreased with lambda phosphatase treatment, suggesting that it is phosphorylated and highly unstable in its dephosphorylated form (Supplementary Figure 9G). GLI1^{FL} and GLI1^{130P}, but not of GLI1^{130}, were detected in a phosphoprotein selected pool, confirming their phosphorylated status (Supplementary Figure 9H).

The kd of p53 in U87 cells increased the levels of GLI1^{130} ~6–8-fold at the expense of GLI1^{130P}. Treatment with λ phosphatase confirmed that GLI1^{130P} is the phosphoform of GLI1^{130} (Figure 7B and D). Endogenous GLI1^{FL} and GLI1^{100} were modestly increased by p53 kd, consistent with the increase in exogenous GLI1^{FL} levels by p53 kd (Figure 5F; Supplementary Figure 9C). Similar results were obtained in glioma D54 (p53 wt) cells (not shown). The data raise the possibility that GLI1^{130P} is a latent and stable form, the conversion of which to its unphosphorylated, labile and active form (GLI1^{130}) is antagonised by p53.

To begin to investigate the mechanisms regulating the balance of GLI1^{130} and GLI1^{130P}, we focused on phosphatase (PP) activity given the suggested involvement of PP2A in Hh signalling (Krishnan *et al*, 1997). U87 and U251 cells were treated with low doses of okadaic acid (OA, 10 nM, 16 h) and extracts subjected to western blotting. OA is a serine/threonine protein phosphatase inhibitor with high affinity for PP2A and much lower affinities for PP1 and PP2B. OA increased (50–80%) GLI1^{130P} in control U87 cells (Figure 7D). In p53 kd cells, which have increased levels of GLI1^{130}, OA treatment reversed the 130P/130 ratio (Figure 7D), decreasing GLI1^{130} by ~40–50% and augmenting GLI1^{130P} ~2-fold. Similar results were obtained in U251 cells (not shown). The very low levels of endogenous GLI1^{FL} prevented us from assessing changes after OA treatment (not shown).

To correlate the levels of GLI1^{130P} with transcriptional activity, endogenous GLI-dependent reporter function was measured in OA-treated U87 cells. OA reduced reporter levels by 60–70% and abolished the increase induced by shp53 (Figure 7E), paralleling the western blot results. Moreover, OA treatment repressed the endogenous levels of both *GLI1* and *PTCH1* mRNAs (Figure 7F), confirming the downregulation of the endogenous HH-GLI pathway.

We also analysed GLI1 isoforms after increasing the strength of HH signalling through kd of the major negative regulators PTCH1 or SUFUH, by RNAi (with *shPTCH1* or *shSUFUH*). Such interference resulted in a ~2.5-fold upregulation of GLI1^{130} at the expense of GLI^{130P} mimicking the effect of p53 kd (Figure 7B and C). Enhanced HH signalling also increased GLI1^{FL} and GLI1^{100} levels by 3–5-fold and 2.5–3-fold, respectively (Figure 7B and C).

These results suggested that OA should inhibit the proliferative effects of enhanced HH pathway activation. The increase in BrdU incorporation in U87 cells driven by *shSUFUH* was reverted by OA treatment (Figure 7G). OA also inhibited untransduced U87 cell proliferation (Figure 7G), which is known to depend on an active HH-GLI pathway (Clement *et al*, 2007). GLI1^{130} thus appears to depend on the action of PP2A or a similar enzyme, being positively regulated by HH signalling and inhibited by p53 (Figure 7H).

The kinases and mechanisms that yield GLI1^{130P} are not known. cAMP-dependent Protein Kinase A (PKA) blocks HH signalling (e.g., Epstein *et al*, 1996), and its enhancement with forskolin (FK), a selective activator of adenyl cyclase, inhibits GLI1 activity (Ruiz i Altaba, 1999; Kaesler *et al*, 2000; not shown). PKA promotes GLI1 phosphorylation and its localisation in the cytoplasm, where it can be degraded (Sheng *et al*, 2006). We therefore tested whether enhanced PKA activity by FK treatment could have the same effect on GLI1^{130} as inhibiting endogenous PP2A and/or similar phosphatase activity by OA. FK treatment of wt U87 cells yielded similar levels of GLI1^{130P} as control or OA-treated cells (Figure 7D). However, FK treatment of cells expressing shp53 did not reverse the GLI1^{130P}/GLI1^{130} ratio to the extent that OA treatment did. Rather, GLI1^{130} was largely eliminated by FK treatment (Figure 7D). The data

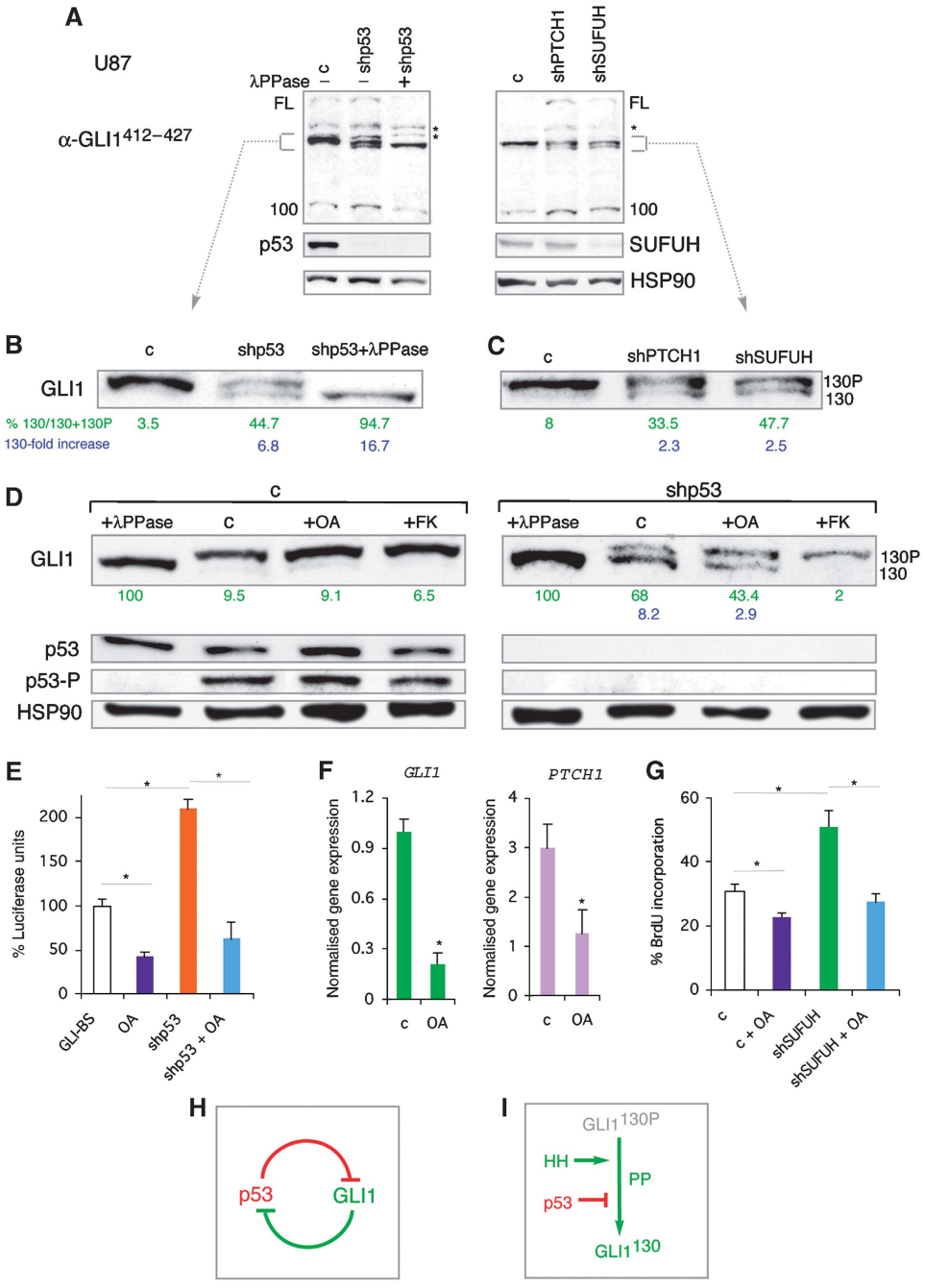

Figure 7 Regulation of GLI1 isoforms and phosphorylation status of GLI1^{130} by p53 and HH signalling. (**A**) Effects of λ phosphatase treatment (+λPPase) or of shp53, shPTCH1 or shSUFUH. Endogenous p53 and SUFUH levels are shown. (**B**, **C**) Enlargements of the ±130 KD area in (A). The %GLI1^{130} calculated by densitometry in relation to total GLI1^{130} + GLI1^{130P} values is green. The fold increase in GLI1^{130}/control is blue. (**D**) Effects of shp53, and of okadaic acid (OA) and forskolin (FK) for 16 h, on GLI1^{130} isoforms in U87 cells. λPPase treatments and p53 and p53-P levels are shown as controls. (**E**) Quantification of endogenous GLI—luciferase assays in control U87 cells and after 16 h OA treatment in wt or shp53-expressing cells. (**F**) RT–qPCR of control and OA-treated U87 cells after 12 h showing decreased expression of *GLI1* ($\times 10^{-4}$) and *PTCH1* ($\times 10^{-3}$). (**G**) Quantification of BrdU incorporation in control and shSUFUH-transduced U87 cells treated or untreated with OA. (**H**) GLI1-p53 inhibitory loop model. (**I**) Proposed regulation of GLI1^{130} by PP2A or a similar enzyme, HH and p53 activities.

raise the possibility that the mechanisms by which PKA antagonises GLI1 activity include the degradation of the GLI1^{130} activator form.

Discussion

Here we show that GLI1 is under negative control by p53 in multiple systems, and that GLI1 and p53 form a novel homeostatic inhibitory loop that normally controls precursor and stem cell numbers. We propose that its modification alters the behavior of stem cell lineages leading to increases or decreases in cell numbers, such as those in cancer or aging, respectively.

The level of GLI1 activity determines brain size and neural stem cell self-renewal

GLI1 is the last mediator of HH signals, acts as a nexus to integrate non-HH signals such as RAS, and is an emerging

central regulator of stemness and cancer in multiple contexts (reviewed in Ruiz i Altaba *et al*, 2007). We find that the level of GLI1 in transgenic mice controls precursor and stem cell numbers in multiple brain regions. Consistent with this, GLI1 induces a stemness signature that includes *Nanog*, *Klf4* and *Sox2*, which parallels that of glioma cancer stem cells (Clement *et al*, 2007) and includes genes involved in reprogramming (Takahashi and Yamanaka, 2006). As the majority of GFP^+ cells in the DT^{+dox} SVZ are not $GFAP^+$, a marker of postnatal semiquiescent stem cells (Doetsch *et al*, 1999), enhanced GLI1 levels could thus increase the number of actively dividing stem cells. Such increases in brain stem cells and precursors are concomitant with the region-specific modulation of several signalling pathways. Notably, GLI1 upregulates Notch and downregulates critical BMP signalling components, in line with the requirement of Notch–Jagged signalling in neural stem cell self-renewal (Nyfeler *et al*, 2005), and the pro-differentiative action of BMP signalling on stem cells (Panchision *et al*, 2001). Moreover, the strong upregulation of Hes1 that we detect *in vivo* and in cerebellar stem cells is consistent with it being a Notch and Gli target (Ingram *et al*, 2008; V Wallace, personal communication) and is interesting in view of its recent implication in the prevention of senescence (Sang *et al*, 2008).

We suggest a role for endogenous Gli1 in neural stem cells as enhanced GLI1 levels expand the number of clonogenic stem cells, and $Prominin1^+$ stem cells from DT^{+dox} cerebella upregulate endogenous *Gli1* while downregulating *Gli2* and *Gli3* (this work). Moreover, even though it is dispensable for mouse development (Park *et al*, 2000), acute interference with endogenous Gli1 in mouse hippocampal NS decreases clone numbers (Galvin *et al*, 2008), and SVZ $Gli1^{-/-}$ mutant mouse NS show a 40% reduction in secondary clonogenicity (M Vukicevic and ARA, personal communication). Gli1 may, therefore, normally contribute to the control of stem cell lineage longevity, acting to balance antagonising p53 function, consistent with the finding that loss of p21, a p53 target, transiently enhances the self-renewal of neural stem cells but then leads to their premature exhaustion (Kippin *et al*, 2005).

The balance of antagonistic GLI1 and p53 functions regulates cell numbers

GLI1 is tightly controlled by multiple mechanisms, and here we show that a novel critical modulator of GLI1 in precursors, stem and tumour cells is p53, a multifunctional tumour suppressor (Harris and Levine, 2005). Our data suggest a model for a novel homeostatic mechanism in which p53 and GLI1 form a regulatory loop (Figure 7H). Here, any inappropriate elevation of GLI1 would induce the DNA damage (replication stress) response, which leads to activation of p53, and elevated p53 would then decrease GLI1 activity. At the same time, however, endogenous GLI1 antagonises endogenous p53, possibly through its regulation of *BMI1* or its activation of the p53 inhibitor Hdm2/Mdm2 (Abe *et al*, 2008; this work).

Normal organ-specific regulation of this loop may act to maintain precursors and stem cells in their appropriate numbers to insure life-long persistence and constant organ size, while preventing tumourigenesis. Interestingly, we found that synergistic enhancement of stem cell numbers by GLI1 and p53 kd increased expression of $p16^{INK4a}$. As increasing $p16^{INK4a}$ levels mark aging neural stem cells (Molofsky *et al*, 2006), such synergistic action may induce neural stem cell aging, possibly leading to their eventual exhaustion, consistent with the self-renewal deficit in NS lacking Gli1 (see above). The p53-GLI1 regulatory loop might thus not only normally act to maintain size and shape, preventing cancer, but might also act to time aging.

Control of GLI1 by p53

Detailed analyses of exogenous and endogenous human GLI1 reveal that GLI1 exists in different forms: $GLI1^{FL}$, $GLI1^{130}$ and $GLI1^{100}$ (Figure 6A), with the first two likely acting as activators and the last one as a weak repressor. $GLI1^{130}$ lacks the N-terminus of $GLI1^{FL}$, and as it is produced from the full-length cDNA, it is distinct from a differential splice form of GLI1 lacking 128aa from the N-terminus (Shimokawa *et al*, 2008). Indeed, this spliced form is exceedingly rare ($\sim$19-fold less abundant than $GLI1^{FL}$ on average in cell lines (Shimokawa *et al*, 2008), whereas $GLI1^{130}$ is $>$10-fold more abundant than $GLI1^{FL}$. The greater abundance of $GLI1^{130}$ over $GLI1^{FL}$ is consistent with the deduced absence in $GLI1^{130}$ of two inhibitory sites in the N-terminus of $GLI1^{FL}$: an N' degron (Huntzicker *et al*, 2006) and a key binding site for the GLI1 antagonist SUFUH (Dunaeva *et al*, 2003).

Our data suggest that p53 acts to inhibit GLI1 function in two ways:

(1) p53 represses the transcriptional activity of $GLI1^{FL}$ by reducing its nuclear localisation and protein levels. This type of regulation is seen with exogenous transfected GLI1 and may be operative with the very rare endogenous $GLI1^{FL}$ protein and possibly with $GLI1^{130}$.

(2) p53 promotes the phosphorylation of the endogenous novel N'Δ $GLI1^{130}$ isoform. We find that $GLI1^{130}$ is predominantly found in a phosphorylated state ($GLI1^{130P}$) and suggest that non-phosphorylated $GLI1^{130}$ is a labile activator, the abundance of which correlates with activity (Figure 7I). Exogenous $GLI1^{FL}$ also appears to be phosphorylated and endogenous $GLI1^{FL}$ might behave similarly, being subjected also to this second mode of regulation.

Concerning the regulation of $GLI1^{130}$, p53 could act, directly or indirectly, to antagonise a protein phosphatase, favouring the inactive and more stable $GLI1^{130P}$. Treatment with low doses of OA increases $GLI1^{130P}$ and decreases $GLI1^{130}$. As OA has a higher affinity for PP2A than to PP1 or PP2B, and the B56ε subunit of PP2A is required for Gli1 function in frog embryos (Rorick *et al*, 2007), the phosphatase responsible for the dephosphorylation of $GLI1^{130P}$ may be PP2A.

The mechanism of N'Δ truncation, phosphorylation site(s) and kinases involved in the genesis of $GLI1^{130P}$ remain to be determined. PKA is an important antagonist of HH signalling (Epstein *et al*, 1996), it inhibits GLI1 activity (Ruiz i Altaba, 1999; Kaesler *et al*, 2000), and we show that activation of endogenous PKA through FK treatment results in the degradation of $GLI1^{130}$. We suggest that although the formation of $GLI1^{130}$ depends on phosphatase activity, its degradation may involve PKA. We also suggest that p53, unlike PKA, acts to antagonise $GLI1^{130}$ by promoting $GLI1^{130P}$.

As activation of HH signalling (by inhibition of PTCH1 or of SUFUH) also modulates and appears to depend on the level and phosphorylation status of $GLI1^{130}$, GLI1 is regulated transcriptionally (Lee *et al*, 1997) and posttranscriptionally by HH signals.

In contrast to the positive role of $GLI1^{130}$, $GLI1^{100}$ might act as an immediate and tonic negative feedback, as it may have

repressor activity and resembles the C'Δ repressor form of GLI3, but unlike this (Pan and Wang, 2007), it is not inhibited by Hh signalling.

It is possible that GLI2 and GLI3 share similarities with the novel regulation of GLI1 we describe here, as N'Δ forms are strong transcriptional activators and Gli2 is an early mediator of Hh signals (Sasaki *et al*, 1999), OA treatment can inhibit Shh signalling (Krishnan *et al*, 1997) and FK treatment phosphorylates Gli2 (Riobó *et al*, 2006).

Imbalance of GLI1 and p53 activities in disease

The homeostatic balance of the GLI1-p53 regulatory loop that we have uncovered appears to be critical. Whereas its imbalance in favour of p53 could affect stem cell lineages and aging (Serrano and Blasco, 2007), imbalance in favour of GLI1 appears to be predominant in cancer and cancer stem cells. For example, glioma cancer stem cells require sustained HH-GLI function (Clement *et al*, 2007) and gliomas frequently lack p53 (e.g., Ohgaki and Kleihues, 2007). We suggest that loss of p53, which is a common event in human cancers, unleashes the normally restricted proliferative and self-renewing activities of GLI1, leading to an expansion of cancer stem cells and derived progenitors. Tumor suppressors may thus normally act to regulate stem cell lineages. In addition to p53 control, the positive regulation of GLI1 activity by the major human oncogenes (RAS, AKT; Stecca *et al*, 2007), and its negative regulation by the tumour suppressor PTEN (Stecca *et al*, 2007), highlights the exquisite regulation of GLI1 activity and provides a rationale for its widespread involvement in human cancer.

Materials and methods

A full account of all methods is given in Supplementary data.

Transgenic mice, neurospheres and cell lines

Doxycycline-regulated *GLI1* transgenic (GFP<-tetO->GLI1) mice were crossed with Nestin->rtTA-IRES-LacZ mice to obtain bigenic mice (Supplementary Figure 1). NS were prepared from brains as in Palma and Ruiz i Altaba (2004), transduced with lentivectors and analysed 4–5 days afterwards.

Plasmids, lentiviral vectors and RNA interference

Transfections were at equimolar amounts unless otherwise specified with pCS2-Myc-tagged human GLI1, GLI1ΔN', GLI2ΔN', GLI3, GLI3R (GLI3C'ΔClaI), frog Gli1, frog NLSGli1 (Ruiz i Altaba, 1999), wt human p53, human dnp53 ($p53^{Thr280}$), pCMV-EGFP or pCMV-LacZ.

Lentiviral vectors were pLV-CTH-shSMOH (Clement *et al*, 2007); pLV-CTH-shPTCH1 with targeting sequence 5′-GCACTATGCTCCTT TCCTC-3′; pLV-WPXL-shp53 (targeting human p53); pLV-Sico-shp53 (targeting mouse p53 Addgene); pLV-KO.1-puro-shSHFUH (Sigma); and pLV-GLI1 was in pLV-Lox-CW or pLV-TWEEN. siRNA sequences for human GLI1 and control siRNA were as described in Sanchez *et al* (2004).

Luciferase reporter assays and isolation of Prominin1$^+$ cells

GLI-binding site luciferase reporter assays were as described in Sasaki *et al* (1999). Cortical and SVZ NS were transfected by nucleofection (Amaxa). Cells of DT^{+dox} and DT^{-dox} brains were dissociated, labelled with Prominin1-microbeads and purified in a magnetic-activated cell-sorting column (Miltenyi Biotec).

Intracranial xenografts and RNA microinjection

Lentivector-transduced U87 human glioblastoma cells (10^5) were grafted using a stereotaxic apparatus (L2,P1,D2 relative to Bregma). Synthetic RNA and MO (Genetools) microinjection into four-cell frog embryos was performed as described in Dahmane *et al* (1997, 2001).

Immunohistochemistry, in situ hybridisation and PCR

Cryostat sections were Xgal stained or immunostained with antibodies as noted. *In situ* hybridisation with digoxygenin-labelled RNA probes was as described in Dahmane *et al* (1997, 2001). Quantitative rtPCR with cDNA was carried out at 60°C using iQTm SYBR green mix (Bio-Rad).

Western blotting

GLI1 protein was detected in westerns with anti-myc tag or anti-GLI1 antibodies and ECL chemiluminescence (Amersham), or SuperSignal West Femto Maximum Sensitivity Substrate (Thermo Scientific) for endogenous GLI1.

Supplementary data

Supplementary data are available at *The EMBO Journal* Online (http://www.embojournal.org).

Acknowledgements

We are grateful to N Dahmane, T Halazonetis and all Ruiz i Altaba laboratory members for discussion; M Vukicevic for p53 sequencing data; C Mas for GLI1 lentivectors; G Zacchetti for technical help; T Halazonetis for antibodies; J Massagué for p53; M Serrano for protocols; D Trono and P Salmon for lentivectors; P Vize for dnp53; N Dahmane for U251 and Daoy cells, and DD Bigner for D54 cells. Grant support was from the NIH-NINDS, SNF, Oncosuisse, and the Louis-Jeantet Foundation to ARA.

References

Abe Y, Oda-Sato E, Tobiume K, Kawauchi K, Taya Y, Okamoto K, Oren M, Tanaka N (2008) Hedgehog signaling overrides p53-mediated tumor suppression by activating Mdm2. *Proc Natl Acad Sci USA* **105:** 4838–4843

Brewster R, Mullor JL, Ruiz i Altaba A (2000) Gli2 functions in FGF signaling during antero-posterior patterning. *Development* **127:** 4395–4405

Clement V, Sanchez P, de Tribolet N, Radovanovic I, Ruiz i Altaba A (2007) HEDGEHOG-GLI1 signaling regulates human glioma growth, cancer stem cell self-renewal, and tumorigenicity. *Curr Biol* **17:** 165–172

Dahmane N, Lee J, Robins P, Heller P, Ruiz i Altaba A (1997) Activation of the transcription factor Gli1 and the Sonic hedgehog signalling pathway in skin tumours. *Nature* **389:** 876–881

Dahmane N, Ruiz i Altaba A (1999) Sonic hedgehog regulates the growth and patterning of the cerebellum. *Development* **126:** 3089–3100

Dahmane N, Sánchez P, Gitton Y, Palma V, Sun T, Beyna M, Weiner H, Ruiz i Altaba A (2001) The Sonic Hedgehog-Gli pathway regulates dorsal brain growth and tumorigenesis. *Development* **128:** 5201–5212

Dennler S, André J, Alexaki I, Li A, Magnaldo T, ten Dijke P, Wang XJ, Verrecchia F, Mauviel A (2007) Induction of sonic hedgehog mediators by transforming growth factor-beta: Smad3-dependent activation of Gli2 and Gli1 expression *in vitro* and *in vivo*. *Cancer Res* **67:** 6981–6986

Doetsch F, Caillé I, Lim DA, García-Verdugo JM, Alvarez-Buylla A (1999) Subventricular zone astrocytes are neural stem cells in the adult mammalian brain. *Cell* **97:** 703–716

Dunaeva M, Michelson P, Kogerman P, Toftgard R (2003) Characterization of the physical interaction of Gli proteins with SUFU proteins. *J Biol Chem* **278:** 5116–5122

Epstein DJ, Marti E, Scott MP, McMahon AP (1996) Antagonizing cAMP-dependent protein kinase A in the dorsal CNS activates a conserved Sonic hedgehog signaling pathway. *Development* **122:** 2885–2894

Farin A, Suzuki SO, Weiker M, Goldman JE, Bruce JN, Canoll P (2006) Transplanted glioma cells migrate and proliferate on host brain vasculature: a dynamic analysis. *Glia* **53:** 799–808

Galvin KE, Ye H, Erstad DJ, Feddersen R, Wetmore C (2008) Gli1 induces G2/M arrest and apoptosis in hippocampal but not tumor-derived neural stem cells. *Stem Cells* **26:** 1027–1036

Gil-Perotin S, Marin-Husstege M, Li J, Soriano-Navarro M, Zindy F, Roussel MF, Garcia-Verdugo JM, Casaccia-Bonnefil P (2006) Loss of p53 induces changes in the behavior of subventricular zone cells: implication for the genesis of glial tumors. *J Neurosci* **26:** 1107–1116

Goodrich LV, Mile L, Higgins KM, Scott MP (1997) Altered neural cell fates and medulloblastoma in mouse patched mutants. *Science* **277:** 1109–1113

Gorgoulis VG, Vassiliou LV, Karakaidos P, Zacharatos P, Kotsinas A, Liloglou T, Venere M, Ditullio Jr RA, Kastrinakis NG, Levy B, Kletsas D, Yoneta A, Herlyn M, Kittas C, Halazonetis TD (2005) Activation of the DNA damage checkpoint and genomic instability in human precancerous lesions. *Nature* **434:** 907–913

Harris SL, Levine AJ (2005) The p53 pathway: positive and negative feedback loops. *Oncogene* **24:** 2899–2908

Huntzicker EG, Estay IS, Zhen H, Lokteva LA, Jackson PK, Oro AE (2006) Dual degradation signals control Gli protein stability and tumor formation. *Genes Dev* **20:** 276–281

Ingram WJ, McCue KI, Tran TH, Hallahan AR, Wainwright BJ (2008) Sonic Hedgehog regulates Hes1 through a novel mechanism that is independent of canonical Notch pathway signalling. *Oncogene* **27:** 1489–1500

Kaesler S, Lüscher B, Rüther U (2000) Transcriptional activity of GLI1 is negatively regulated by protein kinase A. *Biol Chem* **381:** 545–551

Kasper M, Schnidar H, Neill GW, Hanneder M, Klingler S, Blaas L, Schmid C, Hauser-Kronberger C, Regl G, Philpott MP, Aberger F (2006) Selective modulation of Hedgehog/GLI target gene expression by epidermal growth factor signaling in human keratinocytes. *Mol Cell Biol* **26:** 6283–6298

Kato S, Han SY, Liu W, Otsuka K, Shibata H, Kanamaru R, Ishioka C (2003) Understanding the function-structure and function-mutation relationships of p53 tumor suppressor protein by high-resolution missense mutation analysis. *Proc Natl Acad Sci USA* **100:** 8424–8429

Kippin TE, Martens DJ, van der Kooy D (2005) p21 loss compromises the relative quiescence of forebrain stem cell proliferation leading to exhaustion of their proliferation capacity. *Genes Dev* **19:** 756–767

Krishnan V, Pereira FA, Qiu Y, Chen CH, Beachy PA, Tsai SY, Tsai MJ (1997) Mediation of Sonic hedgehog-induced expression of COUP-TFII by a protein phosphatase. *Science* **278:** 1947–1950

Lai K, Kaspar BK, Gage FH, Schaffer DV (2003) Sonic hedgehog regulates adult neural progenitor proliferation *in vitro* and *in vivo*. *Nat Neurosci* **6:** 21–27

Lee A, Kessler JD, Read TA, Kaiser C, Corbeil D, Huttner WB, Johnson JE, Wechsler-Reya RJ (2005) Isolation of neural stem cells from the postnatal cerebellum. *Nat Neurosci* **8:** 723–729

Lee J, Platt KA, Censullo P, Ruiz i Altaba A (1997) Gli1 is a target of Sonic hedgehog that induces ventral neural tube development. *Development* **124:** 2537–2552

Li A, Walling J, Kotliarov Y, Center A, Steed ME, Ahn SJ, Rosenblum M, Mikkelsen T, Zenklusen JC, Fine HA (2008) Genomic changes and gene expression profiles reveal that established glioma cell lines are poorly representative of primary human gliomas. *Mol Cancer Res* **6:** 21–30

Lien WH, Klezovitch O, Fernandez TE, Delrow J, Vasioukhin V (2006) alphaE-catenin controls cerebral cortical size by regulating the hedgehog signaling pathway. *Science* **311:** 1609–1612

Meletis K, Wirta V, Hede SM, Nistér M, Lundeberg J, Frisén J (2006) p53 suppresses the self-renewal of adult neural stem cells. *Development* **133:** 363–369

Molofsky AV, Slutsky SG, Joseph NM, He S, Pardal R, Krishnamurthy J, Sharpless NE, Morrison SJ (2006) Increasing p16INK4a expression decreases forebrain progenitors and neurogenesis during ageing. *Nature* **443:** 448–452

Nguyen V, Chokas AL, Stecca B, Ruiz i Altaba A (2005) Cooperative requirement of the Gli proteins in neurogenesis. *Development* **132:** 3267–3279

Nyfeler Y, Kirch RD, Mantei N, Leone DP, Radtke F, Suter U, Taylor V (2005) Jagged1 signals in the postnatal subventricular zone are required for neural stem cell self-renewal. *EMBO J* **24:** 3504–3515

Ohgaki H, Kleihues P (2007) Genetic pathways to primary and secondary glioblastoma. *Am J Pathol* **170:** 1445–1453

Palma V, Lim DA, Dahmane N, Sánchez P, Brionne TC, Herzberg CD, Gitton Y, Carleton A, Alvarez-Buylla A, Ruiz i Altaba A (2005) Sonic hedgehog controls stem cell behavior in the postnatal and adult brain. *Development* **132:** 335–344

Palma V, Ruiz i Altaba A (2004) Hedgehog-GLI signaling regulates the behavior of cells with stem cell properties in the developing neocortex. *Development* **131:** 337–345

Pan Y, Wang B (2007) A novel protein-processing domain in Gli2 and Gli3 differentially blocks complete protein degradation by the proteasome. *J Biol Chem* **282:** 10846–10852

Panchision DM, Pickel JM, Studer L, Lee SH, Turner PA, Hazel TG, McKay RD (2001) Sequential actions of BMP receptors control neural precursor cell production and fate. *Genes Dev* **15:** 2094–2110

Park HL, Bai C, Platt KA, Matise MP, Beeghly A, Hui CC, Nakashima M, Joyner AL (2000) Mouse Gli1 mutants are viable but have defects in SHH signaling in combination with a Gli2 mutation. *Development* **127:** 1593–1605

Riobó NA, Lu K, Ai X, Haines GM, Emerson Jr CP (2006) Phosphoinositide 3-kinase and Akt are essential for Sonic Hedgehog signaling. *Proc Natl Acad Sci USA* **103:** 4505–4510

Rorick AM, Mei W, Liette NL, Phiel C, El-Hodiri HM, Yang J (2007) PP2A: B56epsilon is required for eye induction and eye field separation. *Dev Biol* **302:** 477–493

Ruiz i Altaba A (1999) Gli proteins encode context-dependent positive and negative functions: implications for development and disease. *Development* **126:** 3205–3216

Ruiz i Altaba A, Mas C, Stecca B (2007) The Gli code: an information nexus regulating cell fate, stemness and cancer. *Trends Cell Biol* **17:** 438–447

Sanchez P, Hernández AM, Stecca B, Kahler AJ, DeGueme AM, Barrett A, Beyna M, Datta MW, Datta S, Ruiz i Altaba A (2004) Inhibition of prostate cancer proliferation by interference with SONIC HEDGEHOG-GLI1 signaling. *Proc Natl Acad Sci USA* **101:** 12561–12566

Sang L, Coller HA, Roberts JM (2008) Control of the reversibility of cellular quiescence by the transcriptional repressor HES1. *Science* **321:** 1095–1100

Sasaki H, Nishizaki Y, Hui C, Nakafuku M, Kondoh H (1999) Regulation of Gli2 and Gli3 activities by an amino-terminal repression domain: implication of Gli2 and Gli3 as primary mediators of Shh signaling. *Development* **126:** 3915–3924

Serrano M, Blasco MA (2007) Cancer and ageing: convergent and divergent mechanisms. *Nat Rev Mol Cell Biol* **8:** 715–722

Sheng T, Chi S, Zhang X, Xie J (2006) Regulation of Gli1 localization by the cAMP/protein kinase A signaling axis through a site near the nuclear localization signal. *J Biol Chem* **281:** 9–12

Shimokawa T, Tostar U, Lauth M, Palaniswamy R, Kasper M, Toftgård R, Zaphiropoulos PG (2008) Novel human glioma-associated oncogene 1 (Gli1) splice variants reveal distinct mechanisms in the terminal transduction of the hedgehog signal. *J Biol Chem* **283:** 14345–14354

Stecca B, Mas C, Clement V, Zbinden M, Correa R, Piguet R, Beermann F, Ruiz i Altaba A (2007) Melanomas require HEDGEHOG-GLI signaling regulated by interactions between GLI1 and the RAS-MEK/AKT pathways. *Proc Natl Acad Sci USA* **104:** 5895–5900

Takahashi K, Yamanaka S (2006) Induction of pluripotent stem cells from mouse embryonic and adult fibroblast cultures by defined factors. *Cell* **126:** 663–676

Wallingford JB, Seufert DW, Virta VC, Vize PD (1997) p53 activity is essential for normal development in Xenopus. *Curr Biol* **7:** 747–757

Wetmore C, Eberhart DE, Curran T (2001) Loss of p53 but not ARF accelerates medulloblastoma in mice heterozygous for patched. *Cancer Res* **61:** 513–516

Yoon JW, Liu CZ, Yang JT, Swart R, Iannaccone P, Walterhouse D (1998) GLI activates transcription through a herpes simplex viral protein 16-like activation domain. *J Biol Chem* **273:** 3496–3501

